

The radio science experiment with BepiColombo mission to Mercury

G. Schettino¹, S. Di Ruzza², F. De Marchi¹, S. Cicalò², G. Tommei¹, and A. Milani¹

¹ Dipartimento di Matematica – Università di Pisa, Largo B. Pontecorvo 5, I-56127 Pisa, Italy, e-mail: gschettino@mail.dm.unipi.it

² SpaceDys s.r.l., Via M. Giuntini 63, I-56023 Navacchio (Pi), Italy

Abstract. BepiColombo is a joint ESA/JAXA mission to Mercury with challenging objectives regarding geophysics, geodesy and fundamental physics. The Mercury Orbiter Radio science Experiment (MORE) is one of the on-board experiments, including three different but linked experiments: gravimetry, rotation and relativity. Using radio observables (range and range-rate) performed with very accurate tracking from ground stations, together with optical observations from the on-board high resolution camera (SIMBIO-SYS) and accelerometer readings from the on-board accelerometer (ISA), MORE will be able to measure with unprecedented accuracy the global gravity field of Mercury and the rotation state of the planet. In this work we present the results of a numerical full-cycle simulation of the gravimetry and rotation experiments of MORE: we discuss the accuracies which can be achieved, focussing in particular on the possible benefits from the use of optical observations in support to the tracking measurements.

Key words. Planets: Mercury – Planets: Radio science – Space missions: BepiColombo

1. Introduction

BepiColombo is an ESA/JAXA mission for the exploration of the planet Mercury (see, e.g., Benkhoff et al. 2010), including two space-crafts, the Mercury Planetary Orbiter (MPO) and the Mercury Magnetospheric Orbiter (MMO), scheduled for launch in 2017 and orbit insertion around Mercury at the beginning of 2024. The Mercury Orbiter Radio science Experiment (MORE) is one of the experiments on-board the MPO spacecraft, devised for improving our understanding of both planetary geophysics and fundamental physics. The main scientific goals of MORE are: to measure the global gravity field of Mercury and its tempo-

ral variations due to tides (*gravimetry experiment*, Milani et al. 2001); to measure the rotation state of the planet, in particular the obliquity and the librations in longitude with respect to the 3:2 spin orbit resonance (*rotation experiment*, Cicalò & Milani 2012); to measure the orbit of Mercury and the propagation of radio waves between Earth and Mercury to test the theory of General Relativity, constraining possible alternative theories of gravitation and providing an improved dynamical model for the Solar System (*relativity experiment*, Milani et al. 2002). Moreover, MORE will perform a very precise orbit determination for the mercurycentric orbit of the space-craft. The described goals will be achieved

thanks to very accurate tracking from ground stations performed with a highly stable multiple frequency radio link in X and Ka bands (see Iess & Boscagli 2001). The radio observables will be supported by two other types of measurements: the strong non gravitational perturbations acting on the spacecraft will be measured by the on-board accelerometer (ISA, Iafolla et al. 2010) and the on-board high resolution camera (HRIC, part of SIMBIO-SYS, see Flamini et al. 2010) will provide optical observations of the planet surface, which can be converted in angular observables to be combined with tracking measurements (range and range-rate).

Despite from a conceptual point of view we cannot separate the three experiments, since they depend in some way one upon the others, in practice, considering the different time scales over which the related phenomena take place, we can separate the gravimetry and rotation experiments on one side and the relativity experiment on the other (see Milani et al. 2001). In this contest, we present a preliminary assessment through the results of a numerical simulation of the gravimetry and rotation experiments of MORE, carried out in an up-to-date realistic scenario.

2. Simulation scenario and generalities

We perform the orbit determination (OD) together with the parameter estimation within a comprehensive software, ORBIT14, developed by the Celestial Mechanics group at University of Pisa¹. The software consists of two main programs: the *data simulator*, which generates the simulated observables (range, range-rate, accelerometer readings, angular observables) and preliminary orbital elements, and the *differential corrector*, which solves for the parameters of interest in a global least squares fit within a constrained multi-arc strategy (see, e.g., Alessi et al. 2012). A detailed discussion on the *differential correction method* used to determine the parameters can be found in Milani & Gronchi (2010), Chapters 5 and 17.

¹ under an Italian Space Agency contract.

2.1. Observables

The simulation scenario consists in a 1 year long simulation, starting on April 10th, 2024 (the actual estimate for spacecraft orbit insertion). The main simulated observables are the tracking data, which consist of range and range-rate measurements. We assume that 2 ground stations are available for tracking, one at Goldstone Deep Space Communications Complex (California, USA) for the Ka-band and the other in Spain, at Cebreros station, for X-band; range measurements are simulated as taken every 120 s, while range-rate every 30 s. We include a gaussian error of $\sigma_r = 30$ cm at 300 s on two-ways range observations and $\sigma_{\dot{r}} = 3 \times 10^{-4}$ cm/s at 1000 s for two-ways range-rate (see Iess & Boscagli 2001).

The other simulated observables are the accelerometer readings and the angular observables from the on-board camera. For the accelerometer, in simulation stage we adopt a simplified model for non gravitational perturbations (see details in Cicaló & Milani 2012) and in differential correction stage we handle the simulated data as they were read by the on-board accelerometer, including also an error model as provided by ISA team². Moreover, in differential correction stage, we introduce a calibration model for systematic effects described by a C^1 spline model. Details can be found in Alessi et al. (2012).

Concerning the camera observables, the starting point is to define a geodetic network on the planet surface by defining 100 reference points on the Mercury surface, chosen randomly but uniformly distributed. We assume the following visibility conditions between each point and the spacecraft: (1) the point has to be illuminated by the Sun, (2) the point has to be in the field of view of the camera. Moreover, only observations of points seen at least twice are considered. When real data will be available, the images taken by the camera will be converted into angular measurements in a non-rotating satellite-centric reference frame. For the purpose of simulations, we assume to already have the angular measurements, without considering the conversion

² private communications.

process. We define an *angular observable* as the pair of angles, ecliptic latitude and longitude, of each point of the network with respect to the spacecraft in a space fixed system at rest with the probe. The angles are then transformed in a mercurycentric inertial reference frame. Moreover, corrections due to the aberration (due to the relative motion of the satellite with respect to Mercury surface) are taken into account. We assume a nadir pointing camera with a total field of view of the camera equal to 1.47° . The error budget includes a nadir pointing error, a star mapper error, an attitude error, thermoelectric deformations, etc.: it is a very complex model, so we replaced it by a very simple one, i.e. by adding a gaussian noise of 2.5 arcsec to the angular observables. This error represents the top accuracy performance.

2.2. Dynamical models

2.2.1. Gravity field of Mercury

The gravity field of Mercury is described by the classical spherical harmonic expansion of the gravitational potential. A static rigid body with mass M and mean radius R , with the center of mass in the origin of the adopted reference frame and with polar coordinates (r, θ, λ) generates a potential U which can be expanded in a spherical harmonics series as:

$$U(r, \theta, \lambda) = \frac{GM}{r} \sum_{\ell=0}^{+\infty} \sum_{m=0}^{\ell} \frac{R^{\ell}}{r^{\ell}} [C_{\ell m} \cos(m\lambda) + S_{\ell m} \sin(m\lambda)] P_{\ell m}(\sin \theta), \quad (1)$$

where $P_{\ell m}(s)$ are the Legendre associated polynomials of degree ℓ and order m and the dimensionless quantities $C_{\ell m}$ and $S_{\ell m}$ are the harmonic coefficients.

The orbit of a satellite around the body contains information about $C_{\ell m}$ and $S_{\ell m}$, and measuring the orbit accurately enough, it is possible to solve for them by a least squares fit. In simulation stage, we included the gravity field of Mercury up to degree and order 25 as measured by the Messenger spacecraft (see Mazarico et al. 2014).

Since the planet Mercury has an elastic component, under the tidal field of the Sun it can be deformed, assuming a bulge shape oriented in the direction of the Sun. This deformation can be described by adding to the potential of Equation (1) a quantity V_L called *Love potential*, Kozai (1965):

$$V_L = \frac{GM_{\odot}k_2R_{\odot}^5}{r_S^3 r^3} \left(\frac{3}{2} \cos^2 \psi - \frac{1}{2} \right), \quad (2)$$

where M_{\odot} and R_{\odot} are the Sun mass and radius, respectively, r_S is the Sun-Mercury distance, r is the Mercurycentric position of the probe and ψ is the angle between r and r_S . The Love number k_2 is the elastic constant which characterizes this effect. In simulation stage we assumed a nominal value $k_2 = 0.25$.

2.3. Rotational state of Mercury

The rotational state of Mercury is mainly determined by two parameters: the obliquity angle η between the spin axis of Mercury and the normal to the orbital plane and the amplitude ε_1 of the librations in longitude at Mercury sidereal period. To define the obliquity angle we introduce two suitable angles, δ_1 and δ_2 , such that:

$$\cos \eta = \cos \delta_1 \cos \delta_2. \quad (3)$$

The gravitational torque of the Sun causes some short period perturbations; the effect of these perturbations is called libration in longitude, which is an oscillation around the secular equilibrium condition of the 3:2 spin-orbit resonance. Introducing the rotation angle φ formed by the direction of the largest physical axis (belonging to the orbital plane) with a reference axis, say the perihelion line, which measures the oscillation about the spin-orbit resonance, we assume that:

$$\begin{aligned} \phi(t) = & \frac{3}{2} n(t - t_p) + \varepsilon_1 \sin(n(t - t_p)) + \\ & + \frac{\varepsilon_1}{\mu} \sin(2n(t - t_p)), \end{aligned} \quad (4)$$

where n is the mean motion of Mercury (88 days), t_p is the time of perihelion and all the quantities refer at J2000 epoch. A detailed analysis of the adopted rotation model

for Mercury can be found in Cicaló & Milani (2012).

In simulation stage we assume as nominal values: $\delta_1 = 4.3$ arcmin, $\delta_2 = 0$, $\varepsilon_1 = 35$ arcsec.

2.4. Relativistic corrections

To determine the orbit of Mercury we adopt a full relativistic model, using a parametric post-Newtonian approach. Details can be found in Milani et al. (2002), Milani et al. (2009), Tommei et al. (2010). For the mercurycentric orbit of the spacecraft we adopt a relativistic multichart approach, in which we solve for the probe equation of motion using, as independent variable, the Mercury proper time (see details in Tommei et al. 2010).

3. Results

After performing the simulation in the scenario detailed above, we solve for the following parameters in a global least squares fit:

- normalized harmonic coefficients $\bar{C}_{\ell m}$ and $\bar{S}_{\ell m}$ of the gravity field of Mercury up to degree and order 25;
- Love number k_2 and rotational parameters $\delta_1, \delta_2, \varepsilon_1$;
- initial conditions of the probe (6 coordinates per arc);
- accelerometer calibrations;
- geodetic coordinates (latitude and longitude) of the reference points defined on the planet surface.

In the following we consider both an analysis based on formal statistics (standard deviations and correlations) as given by the formal covariance matrix and an analysis based on “true” errors, defined as the difference between the value of each parameter at convergence of the differential correction process and the nominal value, used in simulation. In particular, “true” errors represent the real accuracies expected from MORE.

3.1. Gravimetry experiment

The results for the determination of the global gravity field of Mercury can be summarized in Figure 1: we plot the rms value of each harmonic coefficient of the same degree ℓ and the Kaula rule (see Kaula 1966) for comparison, together with the rms value over each ℓ for true errors and formal sigmas.

As it can be seen, we can determine the global gravity field with a signal to noise ratio of several orders of magnitude up to degree $\ell = 15$ and still within a factor 10 up to degree $\ell = 25$. Moreover, the real accuracy defined through the “true” error curve is comparable with the formal one, meaning that in the actual realistic scenario systematic effects due to the accelerometer error model are reasonably absorbed by the calibration process. Finally, comparing the results with the measured accuracies from Messenger (see Mazarico et al. 2014) we find that MORE can significantly improve the knowledge on the gravity field of Mercury: for example, at order $\ell = 2$ we expect an improvement of more than 1 order of magnitude.

3.2. Rotation experiment

The results for the Love number k_2 and the three rotational parameters δ_1, δ_2 (both in arcmin), ε_1 (in arcsec) are shown in Table 1 in terms of formal sigmas and “true” errors. In particular for each parameter we show the result achievable with tracking data alone and the improvement factor attainable including also the angular observables from the on-board camera, defining R_f as the ratio between the formal sigma without camera observables and the formal error including the camera and, similarly, R_t the ratio of “true” error without camera and with it.

The benefit of the combined use of tracking data together with camera observations is evident for almost all the parameters; in general, this result vanishes quickly as soon as we assume a somehow inferior accuracy for angular observables with respect to the nominal 2.5 arcsec gaussian error. Nevertheless, also considering tracking data alone, the expected accuracies from MORE are significantly better

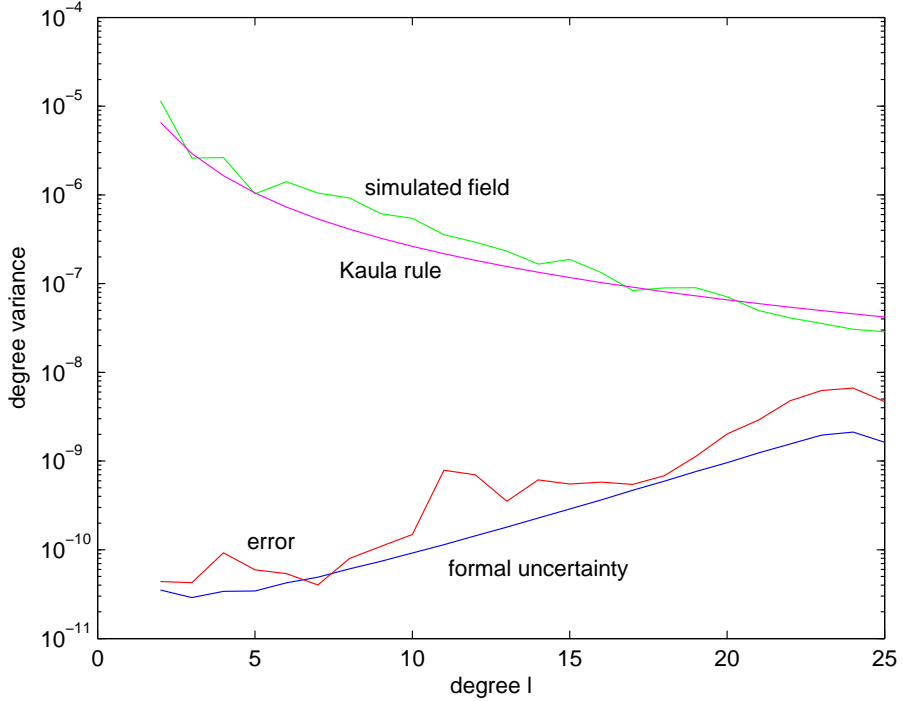


Fig. 1. Gravity field determination: rms values over each degree ℓ of the simulated gravity field (green curve), the Kaula rule (magenta curve), the “true” error (red curve) and the formal uncertainty (blue curve).

Table 1. Love number and rotational parameters results: formal uncertainties and true errors. R_f and R_t are the improvement factors (see text), defined as the ratio between formal or “true” error, respectively, in the case without camera over the case with camera.

Parameter	Formal	R_f	“True”	R_t
k_2	3.3×10^{-4}	1.02	1.7×10^{-4}	1.8
δ_1 [arcmin]	1.8×10^{-3}	2.5	6.8×10^{-4}	5.1
δ_2 [arcmin]	1.1×10^{-3}	1.6	1.2×10^{-3}	1.4
ε_1 [arcsec]	9.6×10^{-2}	1.8	0.65	3.0

than the actual knowledge on each parameter. In fact, k_2 has been estimated by Messenger with an accuracy of 1.4×10^{-2} (see Mazarico et al. 2014) to be compared with our “true” and formal estimates at the 10^{-4} level. The obliquity η has been estimated by Messenger with an accuracy of 0.16 arcmin (see Mazarico et

al. 2014) and by Margot et al. (2012) at the level of 0.08 arcmin, thus our results can produce an improvement of more than one order of magnitude. Finally, the actual uncertainty on ε_1 from Margot et al. (2012) is 1.6 arcsec, hence MORE can improve also the knowledge on this parameter.

4. Conclusions

In this work we have shown the results of a simulation of the MORE gravimetry and rotation experiments, carried out in the up-to-date scenario, including the on-board accelerometer data and the observables from the on-board high resolution camera. In particular, we verified that a significant improvement on the actual knowledge of the rotation state of Mercury can be achieved thanks to the combined use of tracking data and angular observables. Moreover, the results on the determination of the global gravity field of the planet are strongly encouraging, especially comparing them with the actual knowledge from Messenger spacecraft.

Acknowledgements. The results of the research presented in this work have been performed within the scope of the contract ASI/2007/I/082/06/0 with the Italian Space Agency.

References

- Alessi, E. M., Cicalo, S., Milani, A., & Tommei, G. et al. 2012, MNRAS, 423, 2270
- Benkhoff, J., van Casteren, J., Hayakawa, H., et al. 2010, Planet. Space Sci., 58, 2
- Cicaló, S., & Milani, A. 2012, MNRAS, 427, 468
- Flamini, E., Capaccioni, F., Colangeli, L., et al. 2010, Planet. Space Sci., 58, 125
- Iafolla, V., Fiorenza, E., Lefevre, C., et al. 2010, Planet. Space Sci., 58, 300
- Iess, L., Boscagli, G. 2001, Planet. Space Sci., 49, 1957
- Kaula, W.M. 1966, Theory of satellite geodesy (Blaisdell, Walthman, MA)
- Kozai, Y. 1965, PASJ, 17, 395
- Margot, J.L., Peale, S.J., Solomon, S.C., et al. 2012, J. Geophys. Res. (Planets), 117, E00L09
- Mazarico, E., Genova, A., Goossens, S., et al. 2014, J. Geophys. Res. (Planets), 119, 2417
- Milani, A., Rossi, A., Vokrouhlický, D., et al. 2001, Planet. Space Sci., 49, 1579
- Milani, A., Vokrouhlický, D., Villani, D., et al. 2002, Phys. Rev. D, 66, 082001
- Milani, A., et al. 2009, IAU Symposium, 261, 356
- Milani, A., & Gronchi, G.F. 2010, Theory of Orbit Determination (Cambridge Univ. Press, Cambridge, UK)
- Tommei, G., Milani, A., Vokrouhlický, D. 2010, Celest. Mech. Dyn. Astr., 107, 285